

52. IWK

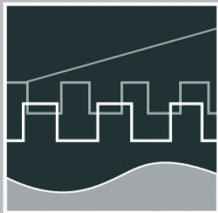
Internationales Wissenschaftliches Kolloquium
International Scientific Colloquium



PROCEEDINGS

| 10 - 13 September 2007

FACULTY OF COMPUTER SCIENCE AND AUTOMATION



COMPUTER SCIENCE MEETS AUTOMATION

VOLUME II

Session 6 - Environmental Systems: Management and Optimisation

**Session 7 - New Methods and Technologies for Medicine and
Biology**

Session 8 - Embedded System Design and Application

Session 9 - Image Processing, Image Analysis and Computer Vision


Session 10 - Mobile Communications

Session 11 - Education in Computer Science and Automation

Bibliografische Information der Deutschen Bibliothek
Die Deutsche Bibliothek verzeichnet diese Publikation in der deutschen Nationalbibliografie; detaillierte bibliografische Daten sind im Internet über <http://dnb.ddb.de> abrufbar.

ISBN 978-3-939473-17-6

Impressum

- Herausgeber: Der Rektor der Technischen Universität Ilmenau
Univ.-Prof. Dr. rer. nat. habil. Peter Scharff
- Redaktion: Referat Marketing und Studentische Angelegenheiten
Kongressorganisation
Andrea Schneider
Tel.: +49 3677 69-2520
Fax: +49 3677 69-1743
e-mail: kongressorganisation@tu-ilmenau.de
- Redaktionsschluss: Juli 2007
- Verlag: 
Technische Universität Ilmenau/Universitätsbibliothek
Universitätsverlag Ilmenau
Postfach 10 05 65
98684 Ilmenau
www.tu-ilmenau.de/universitaetsverlag
- Herstellung und Auslieferung: Verlagshaus Monsenstein und Vannerdat OHG
Am Hawerkamp 31
48155 Münster
www.mv-verlag.de
- Layout Cover: www.cey-x.de
- Bezugsmöglichkeiten: Universitätsbibliothek der TU Ilmenau
Tel.: +49 3677 69-4615
Fax: +49 3677 69-4602

© Technische Universität Ilmenau (Thür.) 2007

Diese Publikationen und alle in ihr enthaltenen Beiträge und Abbildungen sind urheberrechtlich geschützt. Mit Ausnahme der gesetzlich zugelassenen Fälle ist eine Verwertung ohne Einwilligung der Redaktion strafbar.

Preface

Dear Participants,

Confronted with the ever-increasing complexity of technical processes and the growing demands on their efficiency, security and flexibility, the scientific world needs to establish new methods of engineering design and new methods of systems operation. The factors likely to affect the design of the smart systems of the future will doubtless include the following:

- As computational costs decrease, it will be possible to apply more complex algorithms, even in real time. These algorithms will take into account system nonlinearities or provide online optimisation of the system's performance.
- New fields of application will be addressed. Interest is now being expressed, beyond that in "classical" technical systems and processes, in environmental systems or medical and bioengineering applications.
- The boundaries between software and hardware design are being eroded. New design methods will include co-design of software and hardware and even of sensor and actuator components.
- Automation will not only replace human operators but will assist, support and supervise humans so that their work is safe and even more effective.
- Networked systems or swarms will be crucial, requiring improvement of the communication within them and study of how their behaviour can be made globally consistent.
- The issues of security and safety, not only during the operation of systems but also in the course of their design, will continue to increase in importance.

The title "Computer Science meets Automation", borne by the 52nd International Scientific Colloquium (IWK) at the Technische Universität Ilmenau, Germany, expresses the desire of scientists and engineers to rise to these challenges, cooperating closely on innovative methods in the two disciplines of computer science and automation.

The IWK has a long tradition going back as far as 1953. In the years before 1989, a major function of the colloquium was to bring together scientists from both sides of the Iron Curtain. Naturally, bonds were also deepened between the countries from the East. Today, the objective of the colloquium is still to bring researchers together. They come from the eastern and western member states of the European Union, and, indeed, from all over the world. All who wish to share their ideas on the points where "Computer Science meets Automation" are addressed by this colloquium at the Technische Universität Ilmenau.

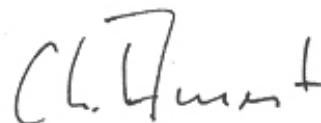
All the University's Faculties have joined forces to ensure that nothing is left out. Control engineering, information science, cybernetics, communication technology and systems engineering – for all of these and their applications (ranging from biological systems to heavy engineering), the issues are being covered.

Together with all the organizers I should like to thank you for your contributions to the conference, ensuring, as they do, a most interesting colloquium programme of an interdisciplinary nature.

I am looking forward to an inspiring colloquium. It promises to be a fine platform for you to present your research, to address new concepts and to meet colleagues in Ilmenau.



Professor Peter Scharff
Rector, TU Ilmenau



Professor Christoph Ament
Head of Organisation

Table of Contents

CONTENTS

	Page
6 Environmental Systems: Management and Optimisation	
T. Bernard, H. Linke, O. Krol A Concept for the long term Optimization of regional Water Supply Systems as a Module of a Decision Support System	3
S. Röhl, S. Hopfgarten, P. Li A groundwater model for the area Darkhan in Kharaa river Th. Bernard, H. Linke, O. Krol basin	11
A. Khatanbaatar Altantuul The need designing integrated urban water management in cities of Mongolia	17
T. Rauschenbach, T. Pfützenreuter, Z. Tong Model based water allocation decision support system for Beijing	23
T. Pfützenreuter, T. Rauschenbach Surface Water Modelling with the Simulation Library ILM-River	29
D. Karimanzira, M. Jacobi Modelling yearly residential water demand using neural networks	35
Th. Westerhoff, B. Scharaw Model based management of the drinking water supply system of city Darkhan in Mongolia	41
N. Buyankhishig, N. Batsukh Pumping well optimi ation in the Shivee-Ovoo coal mine Mongolia	47
S. Holzmüller-Laue, B. Göde, K. Rimane, N. Stoll Data Management for Automated Life Science Applications	51
N. B. Chang, A. Gonzalez A Decision Support System for Sensor Deployment in Water Distribution Systems for Improving the Infrastructure Safety	57
P. Hamolka, I. Vrublevsky, V. Parkoun, V. Sokol New Film Temperature And Moisture Microsensors for Environmental Control Systems	63
N. Buyankhishig, M. Masumoto, M. Aley Parameter estimation of an unconfined aquifer of the Tuul River basin Mongolia	67

M. Jacobi, D. Karimanzira 73
Demand Forecasting of Water Usage based on Kalman Filtering

7 New Methods and Technologies for Medicine and Biology

J. Meier, R. Bock, L. G. Nyúl, G. Michelson 81
Eye Fundus Image Processing System for Automated Glaucoma Classification

L. Hellrung, M. Trost 85
Automatic focus depending on an image processing algorithm for a non mydriatic fundus camera

M. Hamsch, C. H. Igney, M. Vauhkonen 91
A Magnetic Induction Tomography System for Stroke Classification and Diagnosis

T. Neumuth, A. Pretschner, O. Burgert 97
Surgical Workflow Monitoring with Generic Data Interfaces

M. Pfaff, D. Woetzel, D. Driesch, S. Toepfer, R. Huber, D. Pohlers, 103
D. Koczan, H.-J. Thiesen, R. Guthke, R. W. Kinne
Gene Expression Based Classification of Rheumatoid Arthritis and Osteoarthritis Patients using Fuzzy Cluster and Rule Based Method

S. Toepfer, S. Zellmer, D. Driesch, D. Woetzel, R. Guthke, R. Gebhardt, M. Pfaff 107
A 2-Compartment Model of Glutamine and Ammonia Metabolism in Liver Tissue

J. C. Ferreira, A. A. Fernandes, A. D. Santos 113
Modelling and Rapid Prototyping an Innovative Ankle-Foot Orthosis to Correct Children Gait Pathology

H. T. Shandiz, E. Zahedi 119
Noninvasive Method in Diabetic Detection by Analyzing PPG Signals

S. V. Drobot, I. S. Asayenok, E. N. Zacepin, T. F. Sergiyenko, A. I. Svirnovskiy 123
Effects of Mm-Wave Electromagnetic Radiation on Sensitivity of Human Lymphocytes to Ionizing Radiation and Chemical Agents in Vitro

8 Embedded System Design and Application

B. Däne 131
Modeling and Realization of DMA Based Serial Communication for a Multi Processor System

M. Müller, A. Pacholik, W. Fengler Tool Support for Formal System Verification	137
A. Pretschner, J. Alder, Ch. Meissner A Contribution to the Design of Embedded Control Systems	143
R. Ubar, G. Jervan, J. Raik, M. Jenihhin, P. Ellervee Dependability Evaluation in Fault Tolerant Systems with High-Level Decision Diagrams	147
A. Jutmann On LFSR Polynomial Calculation for Test Time Reduction	153
M. Rosenberger, M. J. Schaub, S. C. N. Töpfer, G. Linß Investigation of Efficient Strain Measurement at Smallest Areas Applying the Time to Digital (TDC) Principle	159
9 Image Processing, Image Analysis and Computer Vision	
J. Meyer, R. Espiritu, J. Earthman Virtual Bone Density Measurement for Dental Implants	167
F. Erfurth, W.-D. Schmidt, B. Nyuyki, A. Scheibe, P. Saluz, D. Faßler Spectral Imaging Technology for Microarray Scanners	173
T. Langner, D. Kollhoff Farbbasierte Druckbildinspektion an Rundkörpern	179
C. Lucht, F. Gaßmann, R. Jahn Inline-Fehlerdetektion auf freigeformten, texturierten Oberflächen im Produktionsprozess	185
H.-W. Lahmann, M. Stöckmann Optical Inspection of Cutting Tools by means of 2D- and 3D-Imaging Processing	191
A. Melitzki, G. Stanke, F. Weckend Bestimmung von Raumpositionen durch Kombination von 2D-Bildverarbeitung und Mehrfachlinienlasertriangulation - am Beispiel von PKW-Stabilisatoren	197
F. Boochs, Ch. Raab, R. Schütze, J. Traiser, H. Wirth 3D contour detection by means of a multi camera system	203

M. Brandner Vision-Based Surface Inspection of Aeronautic Parts using Active Stereo	209
H. Lettenbauer, D. Weiss X-ray image acquisition, processing and evaluation for CT-based dimensional metrology	215
K. Sickel, V. Daum, J. Hornegger Shortest Path Search with Constraints on Surface Models of In-the-ear Hearing Aids	221
S. Husung, G. Höhne, C. Weber Efficient Use of Stereoscopic Projection for the Interactive Visualisation of Technical Products and Processes	227
N. Schuster Measurement with subpixel-accuracy: Requirements and reality	233
P. Brückner, S. C. N. Töpfer, M. Correns, J. Schnee Position- and colour-accurate probing of edges in colour images with subpixel resolution	239
E. Sparrer, T. Machleidt, R. Nestler, K.-H. Franke, M. Niebelschütz Deconvolution of atomic force microscopy data in a special measurement mode – methods and practice	245
T. Machleidt, D. Kapusi, T. Langner, K.-H. Franke Application of nonlinear equalization for characterizing AFM tip shape	251
D. Kapusi, T. Machleidt, R. Jahn, K.-H. Franke Measuring large areas by white light interferometry at the nanopositioning and nanomeasuring machine (NPMM)	257
R. Burdick, T. Lorenz, K. Bobey Characteristics of High Power LEDs and one example application in with-light-interferometry	263
T. Koch, K.-H. Franke Aspekte der strukturbasierten Fusion multimodaler Satellitendaten und der Segmentierung fusionierter Bilder	269
T. Riedel, C. Thiel, C. Schmallius A reliable and transferable classification approach towards operational land cover mapping combining optical and SAR data	275
B. Waske, V. Heinzl, M. Braun, G. Menz Classification of SAR and Multispectral Imagery using Support Vector Machines	281

V. Heinzl, J. Franke, G. Menz Assessment of differences in multisensoral remote sensing imageries caused by discrepancies in the relative spectral response functions	287
I. Aksit, K. Bünger, A. Fassbender, D. Frekers, Chr. Götze, J. Kemenas An ultra-fast on-line microscopic optical quality assurance concept for small structures in an environment of man production	293
D. Hofmann, G. Linss Application of Innovative Image Sensors for Quality Control	297
A. Jablonski, K. Kohrt, M. Böhm Automatic quality grading of raw leather hides	303
M. Rosenberger, M. Schellhorn, P. Brückner, G. Linß Uncompressed digital image data transfer for measurement techniques using a two wire signal line	309
R. Blaschek, B. Meffert Feature point matching for stereo image processing using nonlinear filters	315
A. Mitsiukhin, V. Pachynin, E. Petrovskaya Hartley Discrete Transform Image Coding	321
S. Hellbach, B. Lau, J. P. Eggert, E. Körner, H.-M. Groß Multi-Cue Motion Segmentation	327
R. R. Alavi, K. Brieß Image Processing Algorithms for Using a Moon Camera as Secondary Sensor for a Satellite Attitude Control System	333
S. Bauer, T. Döring, F. Meysel, R. Reulke Traffic Surveillance using Video Image Detection Systems	341
M. A-Megeed Salem, B. Meffert Wavelet-based Image Segmentation for Traffic Monitoring Systems	347
E. Einhorn, C. Schröter, H.-J. Böhme, H.-M. Groß A Hybrid Kalman Filter Based Algorithm for Real-time Visual Obstacle Detection	353
U. Knauer, R. Stein, B. Meffert Detection of opened honeybee brood cells at an early stage	359

10 Mobile Communications

K. Ghanem, N. Zamin-Khan, M. A. A. Kalil, A. Mitschele-Thiel Dynamic Reconfiguration for Distributing the Traffic Load in the Mobile Networks	367
N. Z.-Khan, M. A. A. Kalil, K. Ghanem, A. Mitschele-Thiel Generic Autonomic Architecture for Self-Management in Future Heterogeneous Networks	373
N. Z.-Khan, K. Ghanem, St. Leistritz, F. Liers, M. A. A. Kalil, H. Kärst, R. Böringer Network Management of Future Access Networks	379
St. Schmidt, H. Kärst, A. Mitschele-Thiel Towards cost-effective Area-wide Wi-Fi Provisioning	385
A. Yousef, M. A. A. Kalil A New Algorithm for an Efficient Stateful Address Autoconfiguration Protocol in Ad hoc Networks	391
M. A. A. Kalil, N. Zamin-Khan, H. Al-Mahdi, A. Mitschele-Thiel Evaluation and Improvement of Queueing Management Schemes in Multihop Ad hoc Networks	397
M. Ritzmann Scientific visualisation on mobile devices with limited resources	403
R. Brecht, A. Kraus, H. Krömker Entwicklung von Produktionsrichtlinien von Sport-Live-Berichterstattung für Mobile TV Übertragungen	409
N. A. Tam RCS-M: A Rate Control Scheme to Transport Multimedia Traffic over Satellite Links	421
Ch. Kellner, A. Mitschele-Thiel, A. Diab Performance Evaluation of MIFA, HMIP and HAWAII	427
A. Diab, A. Mitschele-Thiel MIFAv6: A Fast and Smooth Mobility Protocol for IPv6	433
A. Diab, A. Mitschele-Thiel CAMP: A New Tool to Analyse Mobility Management Protocols	439

11 Education in Computer Science and Automation

S. Bräunig, H.-U. Seidel Learning Signal and Pattern Recognition with Virtual Instruments	447
St. Lambeck Use of Rapid-Control-Prototyping Methods for the control of a nonlinear MIMO-System	453
R. Pittschellis Automatisierungstechnische Ausbildung an Gymnasien	459
A. Diab, H.-D. Wuttke, K. Henke, A. Mitschele-Thiel, M. Ruhwedel MAeLE: A Metadata-Driven Adaptive e-Learning Environment	465
V. Zöppig, O. Radler, M. Beier, T. Ströhla Modular smart systems for motion control teaching	471
N. Pranke, K. Froitzheim The Media Internet Streaming Toolbox	477
A. Fleischer, R. Andreev, Y. Pavlov, V. Terzieva An Approach to Personalized Learning: A Technique of Estimation of Learners Preferences	485
N. Tsyrelchuk, E. Ruchaevskaia Innovational pedagogical technologies and the Information educational medium in the training of the specialists	491
Ch. Noack, S. Schwintek, Ch. Ament Design of a modular mechanical demonstration system for control engineering lectures	497

V. Heinzel / J. Franke / G. Menz

Assessment of differences in multi-sensoral remote sensing imageries caused by discrepancies in the relative spectral response functions

INTRODUCTION

Spectral vegetation indices derived from satellite observations in the near infrared and visible wavelengths, are widely used within the remote sensing community. Most commonly applied for analysing temporal and spatial vegetation dynamics is the Normalized Difference Vegetation Index (NDVI) [1], defined as:

$$NDVI = \frac{(NIR - RED)}{(NIR + RED)} \quad (1)$$

where RED and NIR denote the spectral reflectance measurements acquired in the red and near-infrared spectrum. Vital green plants absorb solar radiation in the photosynthetically active radiation (PAR) spectral region, which is their source of energy for the photosynthesis process. On the other hand leaf cells scatter (e.g., reflect and transmit) solar radiation in the near-infrared spectral region. The energy level per photon in that domain would result in over-heating the plant and possibly damage the tissues when absorbed. Hence, vital green plants exhibit rather high NDVI values, while diseased vegetation or non-vegetated areas feature rather low or even negative NDVI values (e.g., water).

For multi-temporal vegetation monitoring or change analysis, a combination of multi-sensoral NDVI is often necessary. However, due to different sensor characteristics (e.g., sensor geometry, spatial or radiometric resolution and relative spectral response functions (RSR)) the NDVI can vary. Within this study the focus will be laid on the relative spectral response functions. Whereby, signature variations are introduced because the sensors receive slightly different components of the reflectance spectra of the illuminated target. Several studies have analysed the offset in data products caused by these spectral

characteristics and introduced approaches to minimize those variations [2]-[6].

For the analysis multispectral bands of the satellites Landsat 5 TM, SPOT 5, Aster and QuickBird were simulated by the use of hyperspectral bands from the airborne HyMap sensor. Variations to original satellite data caused by different spatial resolution or other effects are not considered by the sensor simulation and will not be taken into account for the intercalibration process.

After generating each simulated image the NDVI was calculated and the resulting NDVI-varieties were analysed. An empirical cross-calibration method was finally chosen for the intercalibration process.

METHODS AND DATA

Data for sensor simulation

The flight campaign with the airborne Hyperspectral Mapper (HyMap) took place on 28th May 2005 (12.00). HyMap acquires data in 128 bands, with a bandwidth of 15nm in the VIS and NIR region by a geometric resolution of 4m. HyVista corp. and the DLR (German Aerospace Center) carried out the orthorectification and atmospheric correction of the data.

Sensor characteristics of the simulated satellites

Spectral bands are characterized by their spectral range, bandwidth, center wavelength and full width at half maximum (FWHM). The relative spectral response function takes all these features into account and is defined by the effective spectral quantum efficiency (QE) of the detector, including features like the type-dependent sensitivity of the CCD, losses due to light reflecting and transmitting components of the detector (e.g. optics, mirrors, filters, coatings etc.) [7].

Figure 1 illustrates the RSR functions of the different used satellite sensors (Landsat 5 TM, SPOT 5, Aster, QuickBird). The curves differ in shape, central wavelength location and the degree of overlap between the bands. Especially in the region of the red edge (red-NIR translation) (680~800 nm) the sensors vary from each other.

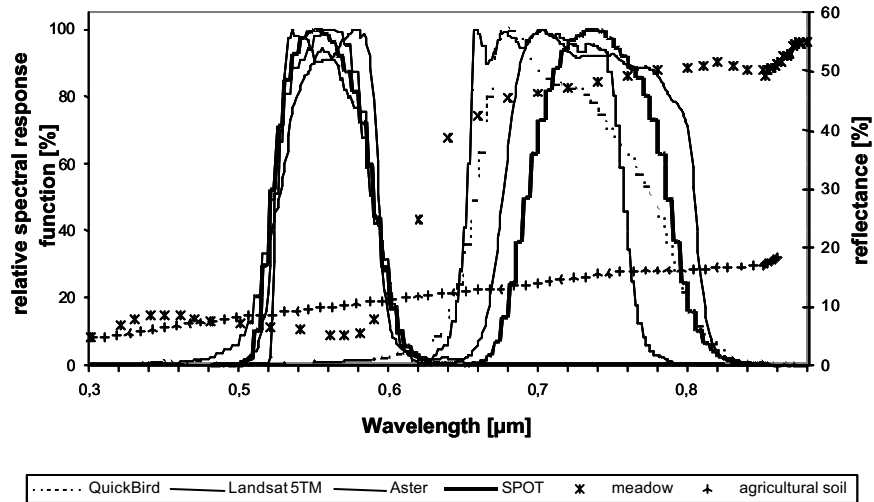


Figure 1. Variations in the red and near-infrared RSR functions among the used earth observing satellites and the spectral profile of two different agricultural targets as reference.

SENSOR SIMULATION

For the differences assessment within the imageries caused by variable RSR-functions the four satellite sensors were simulated using the hyperspectral image. In the first step each HyMap center wavelength was assigned to the mean RSR-value (in the range of FWHM of the hyperspectral band) of the simulating band. In a second step the hyperspectral reflectance values of each pixel were multiplied by the corresponding RSR-values of the simulating band. The sum of these products was then divided by the sum of the band-specific RSR-values. For the multispectral sensor simulation, each band was simulated according to the following equation:

$$R_{sim_b} = \frac{\sum_{i=1}^n R_i * rSR_{b,i}}{\sum_{i=1}^n rSR_{b,i}} \quad 1 \leq n \leq 126 \quad (2)$$

with R_{sim_b} as the simulated pixel reflectance value of the simulated band, R_i pixel reflectance value of the HyMap band and $rSR_{b,i}$ relative spectral response value of the simulating band at each HyMap corresponding wavelength [7].

The validation of the simulation performance was analysed on the basis of a pre-processed Landsat 5 TM scene (28.05.05; 10.30 am) and the simulated Landsat 5 TM image based on an airborne HyMap scene (28.05.05; 12.00 am) [7].

The calculated reflectance and NDVI differences are very marginal with an absolute NDVI difference of 0.626% (Tab. 1). Regarding the real differences between original sensors, they range from 1 ~ 4% for e.g. Landsat 5 TM and Landsat 7 ETM+ [8]. With the marginal differences achieved here, this accurate simulation method is appropriate for analyzing the impact of different RSR functions on the NDVI.

Table 1. NDVI differences between the simulated and the original imagery.

	SIMULATED		ORIGINAL		DIFFERENCE	
	MEAN	STDEV	MEAN	STDEV	absolute	in percent
NDVI	0.635	0.277	0.639	0.258	-0.004	-0.626

NDVI-INTERCALIBRATION

In Table 2 variations between the NDVI of the four simulated sensors are displayed. Differences between SPOT5 and the other sensors feature the widest divergences. Another obvious feature is that the differences between Aster and QuickBird are the smallest both having similar RSR curves.

The general relationships between all sensors can be described as followed. SPOT5 features the highest NDVI values, then Landsat 5 TM, Aster, and the lowest NDVI values exhibits QuickBird.

Table 2. MIN, MAX and MEAN NDVI differences and % difference between the simulated sensors.

	Min NDVI differences	Max NDVI differences	Mean NDVI differences	Differences (%)
SPOT5-Aster	-0.116	0.104	0.012	1.818
SPOT5-Landsat 5TM	-0.157	0.126	0.009	1.364
SPOT5-QuickBird	-0.064	0.099	0.045	7.087
Landsat 5TM-Aster	-0.088	0.091	0.003	0.472
Landsat 5TM-QuickBird	-0.074	0.083	0.013	1.970
QuickBird-Aster	-0.058	0.040	-0.002	-0.322

In general a similar result was found by [4] when trying to model the NDVI inter-sensor relationship. They proposed to model the relationship with a higher polynomial order. The regression coefficients [R^2] for polynomials of different order vary between $R^2= 0.73$ and $R^2= 0.98$ depending on the sensor pairs compared and the order of polynomial. The best correlation results were found for a polynomial of the sixth order.

VALIDATION OF THE NDVI-INTERCALIBRATION

In Table 3 the differences between the sensors after the cross-calibration are displayed. The results for the intercalibration feature a great enhancement in regard to the non-calibrated sensors (Tab. 2). Thus the differences between SPOT5 and QuickBird, which were the biggest difference before intercalibration, decreased from 7.09 % to -0.15 % or 0.16 %, depending on which sensor was taken as the target. Overall, the best results with the smallest bias errors were achieved for translating SPOT5 into Aster and QuickBird. In general the magnitudes of error from translating the sensors into each other lie between -0.15 and 0.61 %, which are good result when comparing it with the results from [3], who reached a precision of 1-2% or [4] with an accuracy of $\sim 2\%$.

When comparing the results of the sixth order intercalibration with the ones of a second order approach [9] it becomes obvious that the sixth order is able to model the differences in a more accurate way. For the second order modeling the NDVI difference after the intercalibration were in the range of -0.91 to 0.80 %, being now significantly smaller.

Table 3. MIN, MAX, MEAN differences and % difference between the original NDVI imagery and the cross-calibrated image. Differences were taken between the original sensor and the cross-calibrated sensor, which is still named after its origin.

original minus cross-calibrated NDVI image	Min NDVI differences	Max NDVI differences	Mean NDVI differences	Mean NDVI differences (%)
SPOT5-Aster	-0.445	0.068	-0.001	-0.152
SPOT5-Landsat 5TM	-0.797	0.106	0.004	0.606
SPOT5-QuickBird	-0.3307	0.052	-0.001	-0.152
Landsat 5TM-Aster	-0.100	0.964	-0.002	-0.315
Landsat 5TM-QuickBird	-0.084	0.910	-0.004	-0.630
Landsat 5TM-SPOT5	-0.107	0.954	-0.003	-0.472
QuickBird-Aster	-0.057	0.031	0.001	0.161
QuickBird-Landsat 5TM	-0.609	0.0784	0.004	0.483
QuickBird-SPOT5	-0.049	0.221	0.001	0.161
Aster-Landsat 5TM	-0.675	0.096	0.002	0.320
Aster-QuickBird	-0.030	0.058	-0.001	-0.160
Aster-SPOT5	-0.067	0.225	-0.001	-0.160

DISCUSSION AND CONCLUSION

The sensor simulation method using airborne hyperspectral data performed well. The residual NDVI differences between the simulated and an original Landsat 5 TM image, added up to only 0.62%. When comparing the simulation result with actually proven discrepancies between different satellite sensors [8] the differences between the simulated

image and an original image were significantly smaller than the actually discovered NDVI differences of 1% to 4%.

The analysed differences in NDVI between the source and target sensors were found to have rather complex patterns, which could be best modelled by sixth order polynomials as supposed by [4] and [9]. The chosen empirical NDVI correction method then performed well, reducing the NDVI differences by 98% for the comparison SPOT5 vs. QuickBird (best case) and by 50% for the relationship QuickBird vs. Aster (worst case). When comparing these results with a second order intercalibration, reducing the differences round 94% for SPOT5 vs. QuickBird or by 5% for QuickBird vs. Aster the sixth order method, performed significantly better [9]. Also when comparing it with the results from [4], who reduced the differences by 80% and 65%, respectively the higher order polynomial performed better. Generally, the results indicate that the NDVI intercalibration is a reasonable first step of a processing chain for multi-sensoral satellite data to ensure the comparability of achieved results.

Acknowledgment

The authors would like to thank Dr. M. Braun from the ZFL for organizing the HyMap flight campaign in Bonn and A. Moll (ZFL) for helping with the IDL programming of the sensor simulation program. The study was realized in the framework of the project ENVILAND (FKZ 50EE0404) funded by the German Aerospace Centre (DLR) and the DFG research training group 722.

References:

- [1] Rouse, J.W., Haas, R.H., Schell, J.A. and Deering, D.W. (1973), Monitoring the vernal advancement and retrogradation (green wave effect) of natural vegetation, Prog. Rep. RSC 1978-1, Remote Sensing Center, Texas A&M Univ..
- [2] Trishchenko, A. P., Cihlar, J. and Li, Z. (2002), Effects of spectral response function on surface reflectance and NDVI measured with moderate resolution satellite sensors. *Remote Sensing of Environment*, 81, 1-18.
- [3] Steven, M.D., Malthus, T.J., Baret, F., Xu, H. and Chopping, M. J. (2003), Intercalibration of vegetation indices from different sensor systems. *Remote Sensing of Environment*, 88, 412-422.
- [4] Miura, T., Huete, A. and Yoshioka, H. (2006), An empirical investigation of cross-sensor relationships of NDVI and red/near-infrared reflectance using EO-1 Hyperion data. *Remote Sensing of Environment*, 100, 223-236.
- [5] van Leeuwen, W.J.D., Orr, B.J., Marsh, S.E. and Herrmann, S.M. (2006), Multi-sensor NDVI data continuity: Uncertainties and implications for vegetation monitoring applications. *Remote Sensing of Environment*, 100, 67-81.
- [6] Franke, J. and Menz, G. (2004), Sensor intercalibration- adjustment of MODISNDVI to AVHRR NDVI data. *International Geoscience and Remote Sensing Symposia*.
- [7] Franke, J., Heinzl, V. and Menz, G. (2006), Assessment of NDVI-differences caused by sensor-specific relative spectral response functions. *International Geoscience and Remote Sensing Symposia*.
- [8] Teillet, P.M., Barker, J.L., Markham, B.L., Irish, R.R., Fedosejevs, G. and Storey, J.C. (2001), Radiometric cross-calibration of the landsat-7 ETM+ and landsat-5 TM sensors based on tandem data sets. *Remote Sensing of Environment*, 78, 39-54.
- [9] Heinzl, V., Franke, J. and Menz, G. (2006), Assessment of cross-sensor NDVI-variations caused by spectral band characteristics. *Proceedings SPIE Vol. 5980, SPIE Remote Sensing*.

Authors:

Dipl. Geogr. Vanessa Heinzl

Dipl. Geogr. Jonas Franke

Prof. Dr. Gunter Menz

ZFL- Center for Remote Sensing of Land Surfaces; Walter-Flex-Str. 3

53113, Bonn, Germany

Phone: +49228-734941

Fax: +49228-736857

E-mail: vheinzel@uni-bonn.de